Synthesis, characterization and photocatalytic activity of titania loaded Cd-MCM-41

Ettireddy P. Reddy, Lev Davydov, and Panagiotis G. Smirniotis *
Department of Chemical Engineering, University of Cincinnati, Cincinnati, OH 45221-0171, USA

Received 11 October 2001; accepted 10 January 2002

Catalysts consisting of cadmium incorporated into MCM-41 mesoporous molecular sieves (Cd-MCM-41) with Si/Cd = 80 have been synthesized by the hydrothermal method using cadmium acetate as the source of cadmium. This was then loaded with titania *via* the sol-gel method to explore the photoactivity in UV light. These two materials were characterized by various physicochemical techniques such as N_2 physisorption, O_2 chemisorption, diffuse reflectance UV-vis, X-ray diffraction (XRD), Raman and X-ray photoelectron spectroscopy (XPS). The pore size of the Cd-MCM-41 was higher and the BET surface area was lower than those commonly found in our siliceous MCM-41. This is due to the partial pore breakage, as recorded by pore size distribution analysis. The oxygen chemisorption results shows that the dispersion of cadmium is quite high, and decreased after loading of titania. The XRD patterns of Cd-MCM-41 and 25%TiO_2/Cd-MCM-41 are similar to those of siliceous MCM-41; however, the intensity of the d_{100} peak is decreased and the unit-cell parameter increased with titania loading. Raman spectra could not detect any peaks, whereas peaks were detected at 144, 397, 518 and 641 cm^{-1} with loading of titania, these peaks being associated with the anatase phase of titania. The surface composition and binding energy of the Cd $3d_{5/2}$ peak for Cd-MCM-41 and 25%TiO_2/Cd-MCM-41 was analyzed by XPS and showed considerable infusion of cadmium ions on to the surface upon loading of titania. The Cd/Si surface atomic ratio measured by XPS increases 10 times with loading of titania on Cd-MCM-41, indicating that the two separate surface electronic levels such as Cd-O-Si and Cd-O-Ti were found for 25%TiO_2/Cd-MCM-41. The 25%TiO_2/Cd-MCM-41 showed higher activity than 25%TiO_2/MCM-41 for photocatalytic degradation of formic acid. The activity results are compared with the pure titania based on the transformation per site of Ti.

KEY WORDS: Cd-MCM-41; 25%TiO_2/Cd-MCM-41; UV-vis; XRD; Raman; XPS; photocatalytic activity; formic acid.

1. Introduction

In the recent past the discovery of silica-based mesoporous molecular sieves M41S, including the hexagonal MCM-41 [1,2], offered new opportunities for creating highly dispersed and more accessible catalytic sites by incorporating transition-metal ions into their silica based frameworks [3–7]. An attempt to incorporate cadmium ions into aluminosilicate Al-MCM-41 during synthesis and by ion exchange was also undertaken [7]. Many of the transition metals incorporated within the framework of mesoporous materials show unique reactivities not only for various catalytic reactions, but also for photocatalytic reactions under UV irradiation [8–10]. Photooxidation by irradiated semiconductors is a relatively new technique for pollution abatement. The vast majority of current studies employ TiO_2 as the semiconductor due to its stability. Cadmium sulfide has also been studied for the photodegradation of organics in visible light, but its stability is very low due to photocorrosion and release of toxic cadmium ions into the reaction medium [11]. Lu and Li [12] have shown that pure CdO does not exhibit any photocatalytic activity for hydrogen production regardless of the method used to prepare this material. Therefore, we decided to incorporate a small amount of cadmium ions inside the framework of MCM-41, load titania to avoid photocorrosion and release of toxic cadmium ions into the reaction medium, and to improve the activity of photocatalytic degradation of formic acid in aqueous medium. There are suggestions in the literature [13] that photocatalytic degradation of formic acid takes place in such a reaction, which produces CO_2 and H_2O directly without any intermediates. Moreover, the titania-loaded Cd-MCM-41 is new system for the photodegradation of formic acid.

In the present study, we have synthesized Cd-MCM-41 and 25%TiO_2/Cd-MCM-41 and characterized by UV-vis, XRD, Raman and XPS techniques for the first time. Photocatalytic degradation of formic acid has also been studied over titania-loaded Cd-MCM-41 and compared with other titania-loaded transition metals (Ti, Mo, Co and Ni) incorporating MCM-41. The important advantage of this titania-loaded Cd-MCM-41 is more active catalysts for photocatalytic degradation of formic acid under mild conditions rather than siliceous MCM-41 reported earlier [8,10] and other titania-loaded transition metals (Ti, Mo, Co and Ni) incorporating MCM-41. Since the other titania-loaded transition metals (Ti, Mo, Co and Ni) do not exhibit any catalytic activity for photodegradation of formic acid, we did not give much importance to these materials. The activity of these

---

* To whom correspondence should be addressed.
E-mail: Panagiotis.Smirniotis@UC.EDU

1011-372X/02/0400-0183/0 © 2002 Plenum Publishing Corporation

catalysts was compared with the pure titania based on the transformation per site of Ti.

2. Experimental

2.1. Synthesis

Cd incorporated MCM-41 with Si/Cd = 80 was prepared by the following procedure. 9.13 g of cetylammonium bromide [Alfa, 99% $CH_3(CH_2)_{15}N(CH_3)_3$] was combined with 20 ml of water and 3.5 ml of ammonium hydroxide (Fisher, 28% NH_4OH) to form solution A; 17.5 ml of LUDOX HS-40 (Aldrich, colloidal silica 40 wt% suspension in water) was combined with 10 ml water and 9.1 ml of tetra-ethylammonium hydroxide to form solution B. A pre-determined amount of solution A and 0.5 g of cadmium acetate [Fisher, 99.87%, $Cd(OCOCH_3)_2 \cdot 2H_2O$] dissolved in 20 ml of water were introduced into solution B under vigorous stirring. After stirring for 30 min at 350 K, the resulting gel was transferred to the oven and kept for 72 h at 373 K under autogenous pressure. The aged gel was washed with deionized water and air-dried. The calcinations of the Cd-MCM-41 to remove the occluded template were carried out in air at *ca.* 823 K for 10 h with the temperature ramp of 2 K/min. The calcined Cd-MCM-41 sample was colorless, indicating the absence of colored CdO species (brown) outside the framework.

The resulting catalyst (typically 1.5 g) was dispersed in ~100 ml of isopropanol, and titanium isopropoxide was added to achieve 25% loading. The system was dried while stirring at ambient temperature. It was then placed in the oven to dry at 100 °C for 1 h, then transferred into a boat-like crucible and calcined at 450 °C for 3 h with a temperature ramp of 2 °C/min.

2.2. BET surface area and pore size distribution

The specific surface area (BET) of the transition metals incorporated MCM-41 and titania-loaded transition metals incorporating MCM-41 materials were measured by nitrogen adsorption at 77 K by the BET method using a Micromeritics Gemini 2360. Horvath–Kawazoe maximum pore volume and adsorption average pore diameter measurements of the supports and the catalysts were performed with a Micromeritics ASAP 2010 using adsorption of N_2 at the temperature of liquid N_2. All samples were degassed at 250 °C under vacuum before analysis.

2.3. Oxygen chemisorption

Oxygen chemisorption measurements were used to study the dispersion of transition metals in the MCM-41. Oxygen uptake measurements of the transition metals incorporated MCM-41 and titania-loaded transition metals incorporating MCM-41 were performed with a Micromeritics ASAP 2010 Chemi system. The known weight of catalysts was taken in a quartz U tube to place the sample and packed with quartz wool below and above the sample. Then this U tube was fixed to the analyzer port of the ASAP Chemi system. The catalysts were reduced in continuous flow of 20 ml/min pure H_2 (Matheson, 99.999%) at 370 °C for 2 h. Subsequently, the reduced catalysts were degassed at the same temperature for 1 h. After evacuation the catalyst was maintained at the same temperature (370 °C) and 20 ml/min pure O_2 (Matheson, 99.999%) gas was passed through the sample to analyze the amount of O_2 adsorption. The stoichiometry factor metal to oxygen is equal to one was used to calculate the dispersion of metal on MCM-41.

2.4. UV-vis spectroscopy

The powders were characterized by a UV-vis spectrophotometer (Shimadzu 2501PC) with an integrating sphere attachment ISR1200 for their diffuse reflectance in the range of wavelengths of 200 to 800 nm. $BaSO_4$ was used as the standard for these measurements.

2.5. X-ray diffraction (XRD)

XRD of Cd-MCM-41 and 25%TiO_2/Cd-MCM-41 was performed by using Nicolet powder X-ray diffractometer equipped with a Cu K_α radiation source (wave length 1.5406 Å) to assess their crystallinity.

2.6. Raman spectroscopy

Raman spectra were obtained at room temperature using an excitation line from Coherent 90-6 Ar^+ (514.5 nm) and K-2 Kr^+ (406.7 nm) ion lasers, collecting backscattered photons directly from the surface spinning (~2000 rpm) solid samples in 8-mm diameter pressed pellets. Conventional scanning Raman instrumentation equipped with a Spex 1403 double monochromator, with a pair of gratings with 1800 grooves/mm, and a cooled photomultiplier detector (Hamamastsu 928) was used to record the spectra under the control of a Spex DM3000 micrometer system. Six scans were done to improve the signal-to-noise ratio. Typically each scan was obtained with a 20 mW laser, the slit width being kept at 6 cm^{-1} for all samples.

2.7. X-ray photoelectron spectroscopy (XPS)

XPS was used to analyze the binding energy values and the atomic surface concentration of corresponding elements on Cd-MCM-41 and 25%TiO_2/Cd-MCM-41 materials. The XPS analyses were conducted on a Perkin-Elmer Model 5300 X-ray photoelectron spectrometer with Mg K_α radiation at 300 W. Typically, 89.45 and 35.75 eV pass energies were used for survey and high-resolution spectra, respectively. The effects of the sample charging were eliminated by correcting the observed spectra for an Si 2p binding energy value of 103.2 eV. The powdered catalysts were mounted on to the sample holder and were degassed overnight at room temperature and pressures of the order of 10^{-7} Torr. The binding energies and atomic concentrations of the catalysts were calculated *via* the XPS results using the total integrated peak areas of the Cd 3d, Ti 2p, Si 2p and O 1s regions.

2.8. Catalysis

The photocatalytic degradation of formic acid was performed to compare the activity on the above catalysts. The photocatalytic studies were carried out in a batch round flat-plate reactor using a 200 W medium pressure mercury lamp (Ace Glass) as the visible light source as described in our earlier paper [8]. The concentration of formic acid was tracked using a conductivity meter (VWR Scientific, cell constant $10\,\mathrm{cm}^{-1}$). The latter device was pre-calibrated for the measurements by standard solutions of formic acid.

3. Results and discussion

The BET surface areas (SA), average pore diameter (APD), and oxygen chemisorption results (% of metal dispersion, MD) are summarized in table 1. One can observe that the presence of Cd metal ions in the gel during synthesis lowers the SA of the resulting MCM-41 material (for example, $\mathrm{SA} = 941\,\mathrm{m}^2/\mathrm{g}$ for siliceous MCM-41 and $\mathrm{SA} = 703.5\,\mathrm{m}^2/\mathrm{g}$ for the Cd-MCM-41 sample). The APD also changes with the introduction of the Cd metal. Since the same surfactant template was utilized for the synthesis of both siliceous and transition metal substituted MCM-41 materials, one should expect to obtain APD in a close range for both types of catalysts. The above discrepancy is therefore due to the partial breakage of the tubular walls of the MCM-41 structure resulting in the formation of bigger pores as well as lower SA.

As shown in table 1, it should be noted that some loss of SA is observed when titania is deposited on the MCM-41 support, as the pore diameters are expected to decrease. Indeed, the APD of MCM-41 also reduces with the loading of titania. This concludes the loss of surface area due to partial blockage of the pores. Similarly, titania-loaded Cd-MCM-41 reduced its surface and pore size distribution. This clearly demonstrates that the titania loading fills up some of the pores leading to their partial blockage, such that the removal of isopropyl alcohol upon calcination does not open the pore mouth.

The results of oxygen chemisorption (% of metal dispersion, MD) are also presented in table 1. Naturally, no MD has been observed for the siliceous MCM-41 sample as well as TiO_2-loaded siliceous MCM-41. However, Cd-MCM-41 exhibited strong oxygen chemisorption. The oxygen chemisorption results also show a pronounced effect of the TiO_2 loading on the MD. For cadmium incorporated MCM-41 about 30% of the MD is lost upon titania loading. This is due to partial blockage of the cadmium ion sites by the TiO_2 loading, making them inaccessible to the reduction of cadmium ions.

Figure 1 shows the diffused reflectance spectra of Cd-MCM-41, 25%TiO_2/Cd-MCM-41 and 25%TiO_2/MCM-41, examined in the range 200–850 nm in order to assess the light absorption characteristics of the catalysts. One can clearly observe that the absorption of UV light is very weak in the case of Cd-MCM-41, the small absorption edge beyond 300 nm may be considered to the CdO, whereas the absorption of UV light is very strong in the case of 25%TiO_2/Cd-MCM-41 followed by TiO_2/MCM-41 when compared to Cd-MCM-41 within the 280–400 nm wavelength region, suggesting that the Cd-MCM-41 was covered by titania. Therefore, these results hint at a possibility that the photocatalytic activity of the titania-loaded Cd-incorporated MCM-41 may be higher than that of the titania-loaded siliceous MCM-41.

The XRD reflections 100, 110, 200 and 210 of Cd-MCM-41 are determined almost at the same location as those of siliceous MCM-41 reflections [1,2], whereas the XRD reflections of 25%TiO_2/Cd-MCM-41 are

Table 1

Physical and physicochemical properties and photocatalytic activity of the catalysts utilized in the study

Catalyst	XRD		Surface area (m^2/g)	Pore size (nm)	Metal dispersion [b] (%)	HCOOH [c] (mM/min)
	d_{100} (nm)	a_0 [a] (nm)				
25%TiO_2/MCM-41	3.61	4.17	667	3.4	0.1	0.011
Cd-MCM-41	3.61	4.17	703	5.2	46.4	0.0007
25%TiO_2/Cd-MCM-41	3.67	4.24	605	3.8	14.7	0.016

[a] Calculated using $a_0 = 2d_{100}/\sqrt{3}$.

[b] Metal dispersion determined by oxygen chemisorption measurement at the stoichiometric factor of metal to oxygen equal to one.

[c] Zero-order reaction rate of UV-assisted photodegradation. Conditions: catalyst, 1 g/l; HCOOH, 10 mM; UV light power, 28 W; oxygen flowrate, 0.5 l/min; T, 300 K.

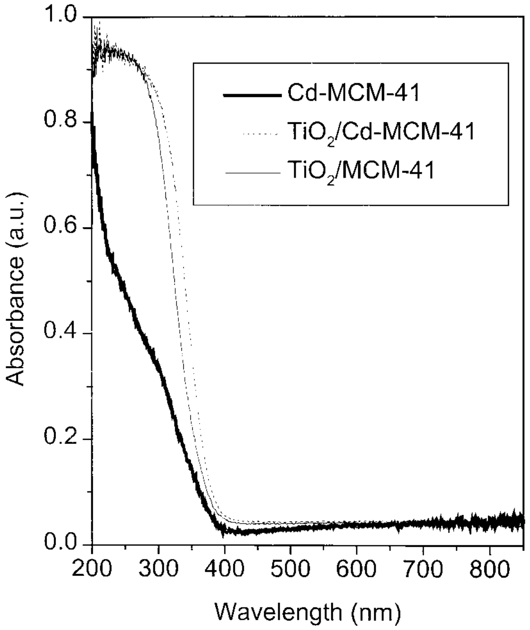

Figure 1. UV-vis diffuse reflectance spectra of the Cd-MCM-41, 25%TiO$_2$/MCM-41 and 25%TiO$_2$/Cd-MCM-41.

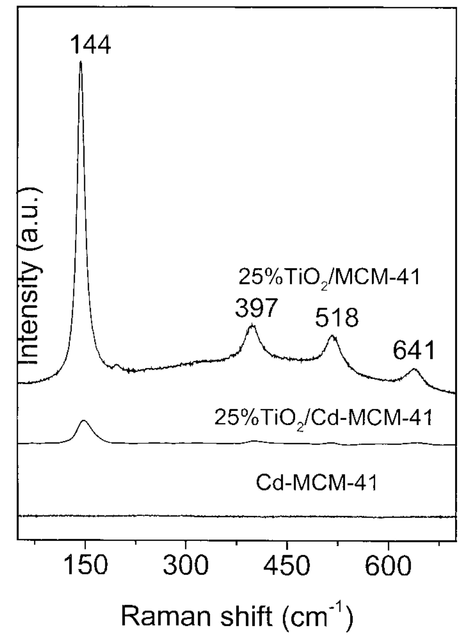

Figure 2. Raman spectra of TiO$_2$/MCM-41, Cd-MCM-41 and 25%TiO$_2$/Cd-MCM-41.

slightly higher than those of the Cd-MCM-41 and siliceous MCM-41. The positions of XRD reflections for Cd-MCM-41 and 25%TiO$_2$/Cd-MCM-41 are indexed to hexagonal lattice structure. The intensities of these peaks lower, when compared to the MCM-41. One can suggest that the presence of Cd ions obstructs the structure-directing action of the template by changing its ionic strength [14]. One more interesting point is that we could not detect any peaks associated to Cd or cadmium oxides. This indicates that the cadmium ions are either dispersed in the MCM-41 framework or stay outside the framework as an amorphous phase. As shown in table 1 the d_{100} and unit cell parameter of Cd-MCM-41 are more than the siliceous MCM-41 [2], which demonstrates that the cadmium is incorporated in the framework of MCM-41. Others [15] also reported that the tungsten was incorporated in MCM-41 frame even though the radius of this ion is bigger than the Cd^{2+}. The XRD of 25%TiO$_2$/Cd-MCM-41 was also recorded in the range of $2\theta = 20^\circ$ to 50° in order to assess the crystallinity of TiO$_2$ loading on to the Cd-MCM-41 and it showed the 25%TiO$_2$/Cd-MCM-41 exhibited low crystallinity of titania. Furthermore, there is increase in the d_{100} by 0.06 nm upon doping of titania on Cd-MCM-41. The d_{100} values and unit-cell parameter of the 25%TiO$_2$/Cd-MCM-41 are listed in table 1. The increase of unit-cell parameter with loading of titania on Cd-MCM-41 demonstrates an intimate contact with cadmium ions and/or uniform distribution of titania on the pore walls of the Cd-MCM-41.

Raman spectra of MCM-41, Cd-MCM-41, 25%TiO$_2$/MCM-41 and 25%TiO$_2$/Cd-MCM-41 are presented in figure 2. Raman spectra associated to Cd-MCM-41 did not show any peaks allied to Si-O, Cd-O bending or stretching modes, shows that the Cd is well dispersed inside the MCM-41 framework. However, in the case of 25%TiO$_2$/MCM-41 and 25%TiO$_2$/Cd-MCM-41, the spectra show four bands at 144, 397, 518 and 641 cm^{-1} indicating the existence of titania (anatase) particles [16]. The intensity of these four peaks are significantly higher in the case of 25%TiO$_2$/MCM-41 than in the case of 25%TiO$_2$/Cd-MCM-41. Therefore, one can easily understand that the loaded titania is directly interacting with the Cd ions incorporated inside the framework of MCM-41.

Cd-MCM-41 and 25%TiO$_2$/Cd-MCM-41 have been investigated by XPS spectroscopy. Table 2 contains the binding energy data for the Cd 3d$_{5/2}$, Cd 3d$_{3/3}$, Si 2p,

Table 2
Binding energy values and surface atomic concentration of Cd-MCM-41 and 25%TiO$_2$/Cd-MCM-41 measured by XPS

Catalyst	Binding energy (eV)				Surface atomic ratios	
	Cd 3d$_{5/2}$	Cd 3d$_{3/2}$	Si 2p	O 1s	Cd/Si	Cd/Ti
Cd-MCM-41	404.6	411.4	103.2	532.4	0.014	ND[a]
25%TiO$_2$/Cd-MCM-41	404.9	411.7	103.2	530 and 532.4	0.14	0.09

[a] ND, not determined.

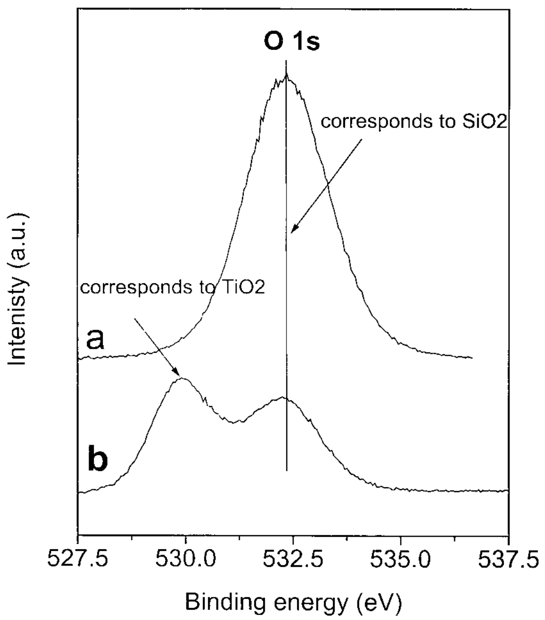

Figure 3. XPS spectra of O 1s core level peak: (a) Cd-MCM-41; (b) 25%TiO_2/Cd-MCM-41.

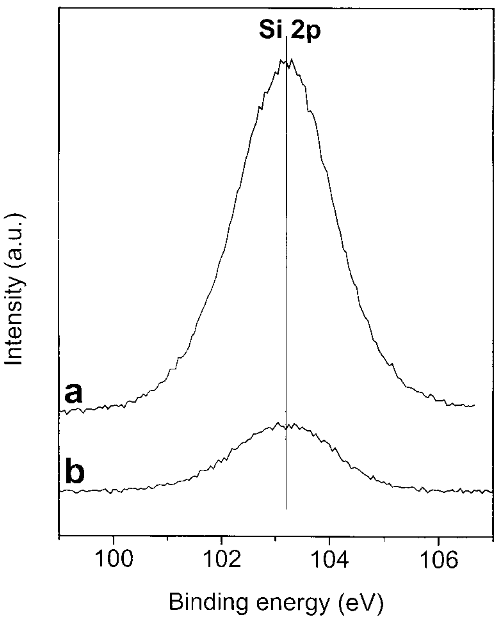

Figure 4. XPS spectra of Si 2p core level peak: (a) Cd-MCM-41; (b) 25%TiO_2/Cd-MCM-41.

Ti $2p_{3/2}$ and O 1s lines and atomic ratios and surface composition of Cd-MCM-41 and 25%TiO_2/Cd-MCM-41 materials. The XPS peaks for O 1s, Si 2p and Cd 3d are presented in figures 3, 4 and 5 respectively.

The XPS spectra of O 1s core level for Cd-MCM-41 and 25%TiO_2/Cd-MCM41 are shown in figure 3. O 1s spectra of Cd-MCM-41 show only one photoelectron peak at 532.4 eV belongs to SiO_2 [17], whereas O 1s spectra of 25%TiO_2/Cd-MCM-41 show two peaks at different binding energy values, which was attributed to the overlapping contribution of oxygen from silica and titania and/or cadmia. As shown in figure 3, one can clearly observe that the O 1s peak at 532.4 eV significantly decreased upon loading of titania on Cd-MCM-41, indicating that the Cd-MCM-41 was covered by loaded titania. The binding energy values of O 1s at 530 and 532.4 eV belong to the oxygen atoms that are bound to TiO_2 [17] and SiO_2, respectively. The appearance of new intense O 1s peak at 530 eV and decreasing of peak intensity at 532.4 eV shows that the titania was dispersed or covered on top of the Cd incorporated MCM-41.

The XPS of the Si 2p core level peak belonging to Cd-MCM-41 and 25%TiO_2/Cd-MCM-41 are shown in figure 4. As shown in table 2, the binding energy value of Si 2p is found at 103.2 eV, which agrees well with the values reported in the literature [18]. The intensity of Si 2p is very high in the case of Cd-MCM-41 when compared to that of 25%TiO_2/Cd-MCM-41. This indicates that the loading of titania is covering the surface of Cd-MCM-41; at the same time, it may also interact with the incorporated cadmium.

Figure 5 shows the core level of the Cd 3d region recorded with Cd-MCM-41 and 25%TiO_2/Cd-MCM-41. A significant increase in the intensity and broadening of the Cd $3d_{5/2}$ line is observed with titania-loaded Cd-MCM-41. The broadening of the XPS peak can be attributed to various factors including (1) the presence of more than one type of Cd ions with different chemical characteristics, which cannot be discerned by XPS, and (2) electron transfer between the incorporated cadmium inside the MCM-41 and loaded titania. The binding energy of Cd $3d_{5/3}$ at 404.6 eV is found for Cd-MCM-41; it probably corresponds to Cd^{2+} which is due to the surface electronic level of Cd-O-Si. The binding energy of Cd $3d_{5/2}$ increased from 404.6 to 404.9 eV

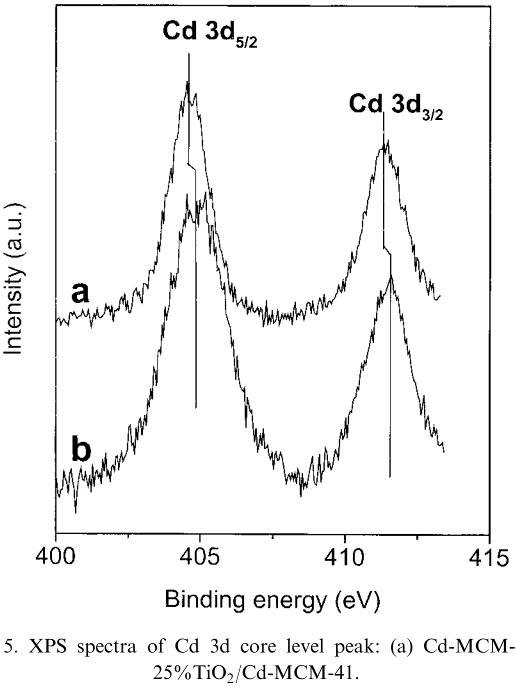

Figure 5. XPS spectra of Cd 3d core level peak: (a) Cd-MCM-41; (b) 25%TiO_2/Cd-MCM-41.

(table 2) upon loading of titania on Cd-MCM-41. The increase of binding energy and the peak intensity of Cd $3d_{5/2}$ predict either the partial breakage of the bond between cadmium and silica and the formation of a new phase called heterojunction between cadmium and titania (Cd-O-Ti) or electron delocalization/transfer between the incorporated cadmium and titania.

The Cd/Si and Cd/Ti surface atomic ratios, as determined by XPS, for Cd-MCM-41 and TiO_2/Cd-MCM-41 materials are shown in table 2. As can be noted from table 2, the Cd/Si atomic ratio is higher for 25%TiO_2/Cd-MCM-41 than for Cd-MCM-41, which indicates that Cd-MCM-41 is covered by TiO_2; at the same time the redistribution of electron levels corresponds to Ti 2p of loaded titania, and Cd $3d_{5/2}$ of incorporated cadmium ions inside the MCM-41 framework may start to interact with each other. Due to this redistribution process the surface of Cd-MCM-41 pore walls enriches with cadmium ions by titania loading. However, the present XPS measurements provide an impression that the incorporated cadmium ions interact preferentially with titania instead of staying inside the framework of the MCM-41 matrix. However, no definite compounds between titania and cadmium are observed from XRD and Raman studies. Nevertheless, the TiO_2/Cd-MCM-41 exhibits more catalytic activity per Ti site for degradation of formic acid, explained below.

As mentioned above, different physicochemical characteristics confirmed that the Cd ion is highly dispersed in the silica-based framework structure of Cd-MCM-41 and 25%TiO_2/Cd-MCM-41 catalysts. The catalytic properties of Cd-MCM-41, 25%TiO_2/Cd-MCM-41, 25%TiO_2/MCM-41 and other transition metals (Ti, Mo, Co, and Ni) incorporating MCM-41 were inspected by carrying out the photocatalytic degradation of formic acid (as an example of organic pollutants) under UV light in an aqueous medium. The concentration of formic acid was analyzed using a conductivity meter (VWR Scientific, cell constant $10\,cm^{-1}$). Titania loaded other transition metals (Ti, Mo, Co and Ni) incorporating MCM-41 catalysts do not exhibit any activity for photocatalytic degradation of formic acid in comparison with TiO_2/Cd-MCM-41 and TiO_2/MCM-41. Therefore, we compared the initial rate of the reaction with respect to 25%TiO_2/Cd-MCM-41 and 25%TiO_2/MCM-41. The initial rate of the reaction over Cd-MCM-41 and 25%TiO_2/Cd-MCM-41 was the same until 15 min of reaction (see figure 6). Surprisingly, the rate of the reaction over 25%TiO_2/Cd-MCM-41 was found to be 1.5 times as fast as that of 25%TiO_2/MCM-41 even after 3 h (table 1). This finding is unique since other researchers postulated that the presence of transition metals in the framework of MCM-41 is deleterious for the activity of titania-loaded MCM-41 catalysts in UV light. The difference of our systems arises from the fact that the transition metal ions (such as cadmium) can diffuse to the surface, thus creating a new energy band. Since the valence band of CdO is lower than that of TiO_2 [19] (+3.2 for CdO and +2.8 for TiO_2 V *versus* NHE), such an arrangement may enhance the oxidation potential of photogenerated holes. Conclusively, our catalytic studies indicate 25%TiO_2/Cd-MCM-41 to be a potentially useful catalyst for degradation of aqueous organic pollutants under UV light.

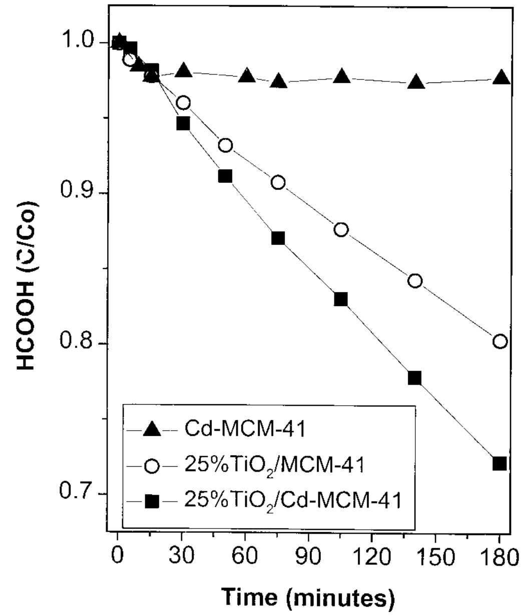

Figure 6. Time course of the degradation of formic acid on the Cd-MCM-41, 25%TiO_2/MCM-41 and 25%TiO_2/Cd-MCM-41 (pH = 6. $T = 25 \pm 3\,^{\circ}C$, catalyst concentration = 1 g/l).

4. Conclusions

The following conclusion can be drawn from this study: the Cd-MCM-41 prepared by hydrothermal treatment method exhibits reasonably high specific surface area, but surface area is decreased and pore size is increased compared to siliceous MCM-41 due to the breakage of pores upon incorporation of Cd. Loading of 25%TiO_2 on corresponding Cd-MCM-41 reduces the surface area and pore size due to the titania coverage on Cd-MCM-41 pores. Characterization of Cd-MCM-41 and 25%TiO_2/Cd-MCM-41 materials by UV-vis, XRD, Raman, XPS and O_2 chemisorption revealed that the cadmium ions are well incorporated inside the framework in the case of Cd-MCM-41; upon loading of titania some Cd is redistributed on to the surface of MCM-41. This redistribution phenomenon is strongly promoted by loaded titania and is accompanied by a loss of specific surface area and average pore diameters. Raman studies of 25%TiO_2/Cd-MCM-41 indicate that the anatase titania phase is present on the surface of the catalysts. The XPS measurements further suggest that some incorporated cadmium interacts preferentially with titania. However, characterization results did not provide evidence about the formation of any specific compound between cadmium and titania. The 25%TiO_2/Cd-MCM-41 is an active catalyst for degradation of formic acid when compared with Cd-MCM-41, 25%TiO_2/MCM-41 and other titania-loaded transition metals (Ti, Mo, Co and Ni) incorporating MCM-41.

Acknowledgments

This work was supported by the United States Department of Army (DOA) through Young Investigator Program (grant DAAD 19-00-1-0399) and NATO (grant SfP-974209). We also acknowledge funding from the Ohio Board of Regents (OBR) that provided matching funds for equipment to the NSF CTS-9619392 grant through the OBR Action Fund #333.

References

[1] C.T. Kresge, M.E. Leonowicz, W.J. Roth, J.C. Vartuli and J.S. Beck, Nature 359 (1992) 710.
[2] J.S. Beck, J.C. Vartuli, W.J. Roth, M.E. Leonowicz, C.T. Kresge, K.D. Schmitt, C.T.-W. Chu, D.H. Olson, E.W. Sheppard, S.B. McCullen, J.B. Higgins and J.L. Schlenker, J. Am. Chem. Soc. 114 (1992) 10834.
[3] R.S. Mulukutla, K. Asakura, S. Namba and Y. Iwasawa, J. Chem. Soc., Chem. Commun. (1998) 1425.
[4] P.T. Tanev, M. Chibwe and T.J. Pinnavaia, Nature 368 (1994) 321.
[5] D. Zhao and D. Goldfarb, J. Chem. Soc., Chem. Commun. (1995) 973.
[6] A. Corma, A. Martinez and V. Martinez-Soria, J. Catal. 169 (1997) 480.
[7] W.Y. Lin, Q.G. Cai, W.Q. Pang and Y. Yue, J. Chem. Soc., Chem. Commun. (1998) 2473.
[8] L. Davydov, E.P. Reddy and P. Smirniotis, J. Catal. (2001) in press.
[9] P. Smirniotis, L. Davydov, E.P. Reddy and P. France, Industrial Applications of Zeolites, 2000, 233–242.
[10] Y.M. Xu and C.H. Langford, J. Phys. Chem. B 101 (1997)
[11] R.V. Khairutdinov, Colloidal J. 59 (1997) 535.
[12] G. Lu and S. Li, J. Photochem. Photobiol. A: Chem. 97 (1996) 65.
[13] R.W. Matthews, Water Res. 24 (1990) 653.
[14] Z. Zhu, Z. Chang and L. Kevan, J. Phys. Chem. B 103 (1999) 2680.
[15] Z.R. Zhang, J.S. Sue, X.M. Zhang and S.B. Li, Appl. Catal. A 179 (1999) 11.
[16] G.T. Went, S.T. Oyama and A.T. Bell, J. Phys. Chem. 94 (1990) 4240.
[17] B.M. Reddy, I. Ganesh and E.P. Reddy, J. Phys. Chem. B 101 (1997) 1769.
[18] C.U.I. Odenbrand, S.L.T. Andersson, L.A.H. Andersson, J.M.G. Brandin and G. Busca, J. Catal. 125 (1990) 451.
[19] P.V. Kamat, Chem. Rev. 93 (1993) 267.